

University of Groningen

Deep Reinforcement Learning for Pellet Eating in Agar.io

Ansó, Nil; Wiehe, Anton; Drugan, Madalina; Wiering, Marco

Published in:

Proceedings of the 11th International Conference on Agents and Artificial Intelligence

DOI:

[10.5220/0007360901230133](https://doi.org/10.5220/0007360901230133)

IMPORTANT NOTE: You are advised to consult the publisher's version (publisher's PDF) if you wish to cite from it. Please check the document version below.

Document Version

Publisher's PDF, also known as Version of record

Publication date:

2019

[Link to publication in University of Groningen/UMCG research database](#)

Citation for published version (APA):

Ansó, N., Wiehe, A., Drugan, M., & Wiering, M. (2019). Deep Reinforcement Learning for Pellet Eating in Agar.io. In *Proceedings of the 11th International Conference on Agents and Artificial Intelligence* (Vol. 2, ICAART, pp. 123-133). SciTePress. <https://doi.org/10.5220/0007360901230133>

Copyright

Other than for strictly personal use, it is not permitted to download or to forward/distribute the text or part of it without the consent of the author(s) and/or copyright holder(s), unless the work is under an open content license (like Creative Commons).

The publication may also be distributed here under the terms of Article 25fa of the Dutch Copyright Act, indicated by the "Taverne" license. More information can be found on the University of Groningen website: <https://www.rug.nl/library/open-access/self-archiving-pure/taverne-amendment>.

Take-down policy

If you believe that this document breaches copyright please contact us providing details, and we will remove access to the work immediately and investigate your claim.

Downloaded from the University of Groningen/UMCG research database (Pure): <http://www.rug.nl/research/portal>. For technical reasons the number of authors shown on this cover page is limited to 10 maximum.

Deep Reinforcement Learning for Pellet Eating in Agar.io

Nil Stolt Ansó¹, Anton O. Wiehe¹, Madalina M. Drugan² and Marco A. Wiering¹

¹*Bernoulli Institute, Department of Artificial Intelligence, University of Groningen, Nijenborgh 9, Groningen, Netherlands*

²*ITLearns.Online, Utrecht, Netherlands*

Keywords: Deep Reinforcement Learning, Computer Games, State Representation, Artificial Neural Networks.

Abstract: The online game Agar.io has become massively popular on the internet due to its intuitive game design and its ability to instantly match players with others around the world. The game has a continuous input and action space and allows diverse agents with complex strategies to compete against each other. In this paper we focus on the pellet eating task in the game, in which an agent has to learn to optimize its navigation strategy to grow maximally in size within a specific time period. This work first investigates how different state representations affect the learning process of a Q-learning algorithm combined with artificial neural networks which are used for representing the Q-function. The representations examined range from raw pixel values to extracted handcrafted feature vision grids. Secondly, the effects of using different resolutions for the representations are examined. Finally, we compare the performance of different value function network architectures. The architectures examined are two convolutional Deep Q-networks (DQN) of varying depth and one multilayer perceptron. The results show that the use of handcrafted feature vision grids significantly outperforms the direct use of raw pixel input. Furthermore, lower resolutions of 42×42 lead to better performances than larger resolutions of 84×84 .

1 INTRODUCTION

Reinforcement learning (RL) is a machine learning paradigm that uses a reward function that assigns a value to a specific state an agent is in as a supervision signal (Sutton and Barto, 2017). The agent attempts to learn what actions to take in an environment to maximize this reward signal. The environment for this research is based on the game of Agar.io, which is itself inspired by the behaviour of biological cells. The player controls circular cells in a 2D plane (as if laid out on a Petri dish) which follow the player's mouse cursor. The player can signal their cells to split or eject little vesicles of mass. Cells of a player can eat small food pellets scattered in the environment or other smaller enemy player-controlled cells to grow in size. The environment of Agar.io is therefore very interesting for RL research, as it is mainly formed by the behavior of other (larger) players on the same plane, it is stochastic and constantly changing. Also the output space is continuous, as the cells of the player move towards the exact position of the mouse cursor. On top of that, the complexity of the game can be scaled by introducing or removing additional features. This paper therefore studies how to use RL to build an intelli-

gent agent for this game, especially focusing on how to represent the game state for the agent.

The use of artificial neural networks (ANN) has demonstrated great promise at learning representations of complex environments. Tesauro was among the first to show that near-optimal decision making could be learned in the large state space of the game Backgammon through the use of a multilayer perceptron (MLP) and temporal difference learning (Tesauro, 1995). Over the years, this principle has been extended through the use of convolutional neural networks (CNNs). This has been shown to achieve human level performance by learning from solely pixel values in a variety of Atari games (Mnih et al., 2013), and even first-person perspective 3D games like Doom (Lample and Chaplot, 2017).

A problem of directly learning from pixel values is that the state spaces are extremely large, which results in large computational requirements. One approach to overcoming the issue of large state spaces is by pre-processing the game state in order to extract features that boost performance and reduce the amount of potentially irrelevant information required for the network to process. The use of vision grids is one such approach that has been employed in games such as

Starcraft (Shantia. et al., 2011) and Tron (Knegt et al., 2018) by extracting hand-crafted features into grids. Such methods can greatly simplify the state space and allow for a decreased network complexity. Despite this benefit, feature extraction might introduce biases and has no guarantee to achieve the same performance as a network being fed the raw game representation (given enough training time).

A widely successful algorithm for reinforcement learning that acts on state representations is Q-Learning (Watkins, 1989). This algorithm can be combined with a function approximator to estimate the Quality, or long-term reward prospect, of a state-action pair. This algorithm has been used in the research mentioned above on Atari games (Mnih et al., 2015), Doom (Lample and Chaplot, 2017), and Tron (Knegt et al., 2018). In Atari games, Doom and Tron, the possible actions in each state are equivalent to the buttons that the player can press. In Agar.io, the relative position of the mouse cursor on the screen is used to direct the player. This has a range of continuous values, similarly to real-life robotic actuators, which are therefore discretized in this work.

Contributions of this Paper. This paper explores how the complexity of the state space affects the convergence and final performance of the reinforcement learning algorithm. This is explored through a core task of the game: pellet collection. In this task, the agent has to navigate in the environment and eat as many food pellets as possible.

More specifically, this research focuses on how different state representations, varying resolutions of such state representations, and varying the structure of the function approximators affect the performance of the Q-learning algorithm. First, different kinds of low-level information used in the state representation are compared, each one providing a different kind of information. This includes grayscale pixel values, RGB pixel values, and a semantic vision grid for pellets in the environment. The effect of the resolution of these state representations is also explored. Finally the ability of Q-learning to achieve a good playing performance is examined when using two different CNN structures (which differ in the number of layers) which are also compared to the use of an MLP.

Paper Outline. Section 2 outlines the fundamental principles behind Q-learning combined with ANNs and the techniques used to enhance its performance. In Section 3, the game of Agar.io and the different state representations are described. The experimental setup follows in Section 4, where the network structures and other experimental parameters are described. Next, Section 5 shows and discusses the experimental results. Section 6 gives the conclusions.

2 REINFORCEMENT LEARNING

This paper follows the general conventions (Sutton and Barto, 2017) to model the reinforcement learning (RL) problem as a Markov decision process (MDP). In a Markov Decision Process an agent can take an action in a state to get to a new state, for which it receives a scalar reward. The transition from the state to the new state has the Markov property: the stochastic transition probabilities between the states are only dependent on the current state and selected action.

To model the RL problem as an MDP, it must be defined what a state constitutes of. In short, the state consists of the properties the environment has and how the agent perceives the available relevant information. The transition between a state and an action to a new state is handled by the game engine.

2.1 The Reward Function

In RL there must be some function that maps a state transition to a reward, also called the reward function. The aim of the agent in RL is to maximize the total expected reward that the agent receives in the long run through this reward function, also called the gain (G):

$$G = \sum_{t=0}^{\infty} r_t \cdot \gamma^t \quad (1)$$

r_t indicates the reward the agent receives at time t and γ indicates the discount factor. This discount factor is a number between 0 and 1 and controls how much future rewards are discounted and therefore how much immediate rewards are preferred.

2.2 Q-Learning

Q-learning (Watkins, 1989) predicts the quality (Q-value) of an action in a specific state. By iterating through all possible actions in a state, the algorithm picks the action with the highest Q-value as the action that the agent should take in that state. The Q-value indicates how much reward in the long term, or how much gain, the agent can expect to receive when choosing action a in state s . This prediction is updated over time by shifting it towards the reward that the agent got for taking that action and the predicted value of the best possible action in the next state.

As Q-learning iterates over all possible actions in a state, the action space cannot be continuous. Therefore we discretize the action space by laying a grid of actions over the screen (Figure 1). Every center point of a square in the grid indicates a possible mouse position that the algorithm can choose.

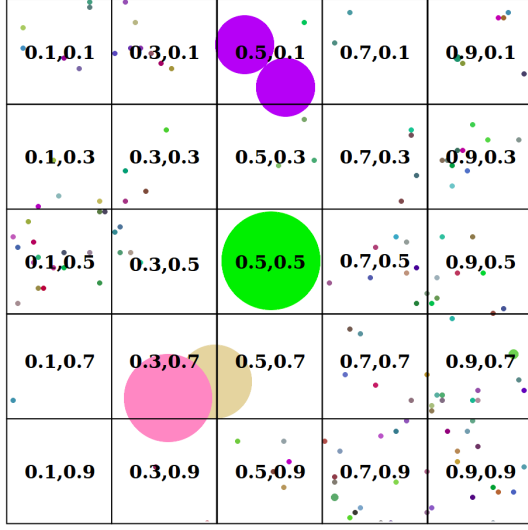


Figure 1: Possible action coordinates are laid out in a grid-like fashion. At a given state, the network chooses the square with the highest Q-value as an action. In total, there are 25 possible actions.

To predict the Q-value for an action in a state, an artificial neural network (ANN) is used, which is trained through backpropagation. To construct the ANN to predict the Q-values we took inspiration from the network structure proposed in (Mnih et al., 2013). This architecture feeds the state as an input to the network and has one output node per possible action. The tabular Q-learning update for a transition from state s_t after selecting action a_t with reward r_t and the new state s_{t+1} is:

$$Q(s_t, a_t) = Q(s_t, a_t) \cdot (1 - \alpha) + \alpha \cdot (r_t + \gamma \cdot \max_a Q(s_{t+1}, a))$$

In this formula α indicates the learning rate. This formula is adapted so that it can be used to train an ANN by calculating the target for backpropagation for a specific state-action pair (s_t, a_t) :

$$Target(s_t, a_t) = r_t + \gamma \cdot \max_a Q(s_{t+1}, a) \quad (2)$$

2.2.1 Exploration

It is necessary to explore the action space throughout training to avoid being stuck in local optima. For Q-learning the ϵ -greedy exploration (Sutton and Barto, 2017) was chosen due to its simplicity. The ϵ value indicates how likely it is that a random action is chosen, instead of choosing greedily the action with the highest Q-value. For this research the ϵ value is annealed exponentially from 1 to a specific value close

to 0 over the course of training. The ϵ value should decrease over time, as this allows the agent to progress more in the game by taking more greedy actions. This causes the agent to progress steadily while exploring alternative actions over the course of training.

2.2.2 Target Networks

To stabilize Q-learning when combined with artificial neural networks, (Mnih et al., 2013) introduced target networks. As Q-learning computes targets by maximizing over the possible actions taken in the next state, the combination of this algorithm with function approximators can lead to the deadly triad (Sutton and Barto, 2017). This deadly triad gives a high probability of the Q-function to diverge from the true function over the course of training. A possible remedy to this problem is Double-Q-learning (Hasselt, 2010), which uses two Q-value networks. For the training of one network, the other network is used to calculate the Q-value of the action in the next state of a transition to avoid the positive feedback loop of the deadly triad. Mnih et al. simplify this approach by introducing a target network in addition to the Q-value network. The parameters of the Q-value network are copied to the target network every time after a certain amount of steps. This requires no need to train a new separate network, but the maximization of the Q-values is still done by a slightly different network, therefore mitigating the unwanted effect.

2.2.3 Prioritized Experience Replay

Lin introduced a technique named experience replay to improve the performance of Q-learning (Lin, 1992). The technique has been shown to work well for DQN (Mnih et al., 2015). When using experience replay every transition tuple (s_t, a_t, r_t, s_{t+1}) is stored in a buffer instead of being trained on directly. If this buffer reaches its maximum capacity the oldest transitions in it get replaced. To train the value network using experience replay in every training step N random transitions (experiences) from the replay buffer are sampled with replacement to create a mini-batch. For each of the transitions in the mini-batch the target for s_t and a_t is calculated and then the value network is trained on this mini-batch.

This form of experience replay offers a big advantage over pure online Q-learning. One assumption of using backpropagation to train an ANN is that the samples that are used to train in the mini-batches are independent and identically distributed. This assumption does not hold for online Q-learning, as each new transition is correlated with the previous transition. Therefore random sampling from a large buffer

of transitions partially restores the validity of this assumption. Furthermore, with experience replay, experiences are used much more effectively, as the agent can learn multiple times from them.

As an enhancement of experience replay, prioritized experience replay (PER) has been introduced (Schaul et al., 2015). PER does not sample uniformly from the replay buffer, but instead assigns the sampling probability to an experience i :

$$P(i) = \frac{TDE_i^\alpha}{\sum_k TDE_k^\alpha} \quad (3)$$

Here, the α coefficient determines how much prioritization is used, $\alpha = 1$ would mean full prioritization. TDE stands for the temporal difference error of transition i , computed as:

$$TDE_i = r_t + \gamma \cdot \max_a Q(s_{t+1}, a) - Q(s_t, a_t) \quad (4)$$

This implies that the badly predicted transitions are replayed more often in the network, which was shown to lead to faster learning and better final performance (Schaul et al., 2015).

More transitions with high TDEs trained on in PER leads to proportionally larger changes in the weights of the network. Schaul et al. introduced an importance sampling weight which decreases the magnitude of the weight change in the MLP for transition i anti-proportionally to its TDE_i . This is done to reduce the bias of training on average on more high TDE transitions. Therefore, a weight w_i is applied to the weight changes induced by each transition i of magnitude:

$$w_i = \left(\frac{1}{N} \cdot \frac{1}{TDE_i} \right)^\beta \quad (5)$$

In this formula N is the batch size and β controls the amount of applied importance sampling. In practice the weights are used in the Q-learning update by multiplying the prediction error for transition i , used in backpropagation, by w_i .

3 THE GAME AND STATE REPRESENTATION

Agar.io is a multi-player online game in which the player controls one or more cells. The game has a top-down perspective on the map of which the size of the visible area of the player is based on the mass and count of their cells. The goal of the game is to grow a player as much as possible by absorbing food pellets, viruses, or other smaller enemy player's cells. The game itself has no end. Players can join an ongoing game at any point in time. Players start the game as a

single small cell in an environment with other player's cells of all sizes. When all the cells of a player are eaten, that player loses and may choose to re-enter the game.

In every time step, every cell in the game loses a small percentage of its mass. This makes it harder for large cells to grow quickly and it punishes inaction or hesitation. The game has simple controls. The cursor's position on the screen determines the direction all of the player's cells move towards. The player also has the option to 'split', in which case every player cell (given the cell has enough mass) splits into two cells of the same mass, both with half the mass of the original cells. Furthermore, the player has an option to have every cell 'eject' a small mass blob, which is eaten by other cells or viruses. Although, the game has relatively simple core mechanics, the game also has a complex and dynamic range of environments. The larger a cell is, the slower it moves. This forces players to employ strategies with long-term risks and rewards.

For the purpose of this research, the game was simplified to fit the computational resources available. The used version of the game has disabled viruses and runs with only one player. Furthermore, ejecting and splitting actions were disabled for the experiments in this paper. Ejecting is only useful for very advanced strategies, and splitting requires tracking of when the player's cells are able to merge back together over long time intervals. The use of these actions would require recurrent neural networks such as LSTMs (Hochreiter and Schmidhuber, 1997) which are outside of the scope of this research. Figure 2 shows a screenshot of the developed clone of Agar.io used for this research.

We also introduce a 'Greedy' bot to the game to compare against the RL agents. This bot is pre-programmed to move towards the cell with the highest cell mass to distance ratio. The bot ignores cells with a mass above its biggest own cell's absorption threshold. The bot also has no splitting or ejecting behavior. This relatively naive heuristic, outperforms human players at early stages of the game. On the other hand, the heuristic is often outperformed later in the game by abusing its lack of path planning and general world knowledge.

The aim in Agar.io is to grow as big as possible. That means the agent has the aim to maximize the mass of its cell in the shortest amount of time possible. This leads to the idea of the reward being the change in mass (m) between the previous state and the current state:

$$r_t = \begin{cases} 0, & \text{if } t = 0 \\ m_t - m_{t-1}, & \text{otherwise} \end{cases} \quad (6)$$

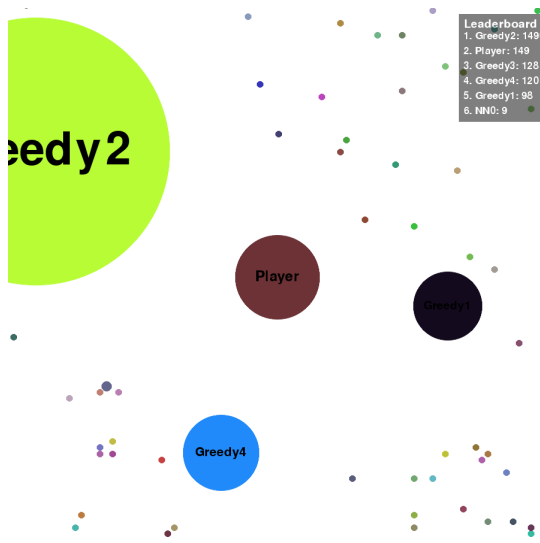


Figure 2: A clone of the game Agar.io used for this research. The player has one cell in the center of the screen. This player is in danger of being eaten by the Greedy bot seen on the top left, the other cells have a similar size as the player’s cell and therefore pose no danger. The little colored dots are pellets that can be consumed to grow in mass.

This research applies frame-skipping to the MDP. In frame skipping a certain number of frames, or states, are skipped and the action that the agent chose is applied during all of these skipped frames. Also the rewards during these skipped frames are summed up until the next non-skipped state where the sum total is used as the reward. Frame skipping offers a direct computational advantage, as it allows the agent to not have to calculate the best action in every single frame of the game. More importantly, frame skipping leads to successive states in the MDP to be more different from each other than without frame skipping and leads to higher rewards, simply because more steps happened in between states. Making successive states more different from each other makes it easier for a function approximator to differentiate states. Larger and more different rewards also have a positive effect on the training speed.

3.1 The State Representation

The information used in state representations can have varying levels of abstraction. The choice of a given state representation often brings positive and negative influences on the algorithm’s learning process, which the designer has to balance optimally. State representations with high levels of abstraction usually have the environment information preprocessed before it is fed to the algorithm. This has the advantage of allowing for a simpler network which

takes less training time to converge. However, state representations of hand-crafted features are inherently biased due to being created with the programmer’s own heuristic in mind. An example of this is Bom et al.’s paper on learning to play Ms. Pac-Man (Bom et al., 2013), where a small neural network learns to play the game by using a representation that includes the distance to the closest collectable pills as determined by an A* search algorithm.

On the other end of the spectrum there are approaches where the unfiltered raw data of the environment is fed to the learning algorithm. The simplicity of this approach allows for agents to learn in complex state-action spaces for which humans might have non-optimal existing heuristics. The downside is that the large number of parameters the networks are required to have, brings issues with processing power and amount of training time before convergence.

One of the aims of this paper is to research how state representations of the same resolution, but with varying levels of preprocessing compare to one another. The base representation of the game is the raw state representation of the game, which comes in the form of *RGB pixel values*. The second state representation uses the *grayscale pixel values*. A player in Agar.io aims to locate food pellets and cells in its view against a white background. Processing the RGB channels into a single grayscale channel reduces the amount of weight tuning required for the network in order to extract non-white objects. This processing is performed by a pixel-wise averaging across the RGB channels. The third state representation is a *semantic representation* of objects in the environment. This consists of a vision grid in which every individual area unit has a value equal to the amount of food pellets contained in that area (see Figure 3). For the following experiments, the grid values at given areas were obtained from the game engine itself to reduce computational costs, but one could theoretically obtain these values from the RGB pixel values of the real game using preprocessing techniques.

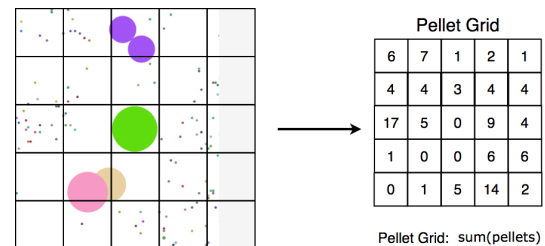


Figure 3: The semantic state representation consists of a vision grid laid out on the player’s view. Values are then extracted from each area unit based on how many food pellets are present in it. Note that in the pellet eating task, the learning agent is the only player in the game.

Another aim of this paper is to explore how much the performance is influenced by the resolution of these representations. The DQN approach has shown success with state representation sizes of 84 by 84 (Mnih et al., 2015), but one could hypothesize that as the representation resolution drops, it will be harder for the network to understand the specific situation of the game. Given this, semantic representations should be expected to perform marginally better than pixel values at lower resolutions.

The last aim of this paper is to compare how different representations perform with different architectures. Every subsequent layer in a neural network can be thought of as providing recognition of more abstract concepts. Providing the network with a more semantically complex state representation to begin with, might relieve the network from the need to extract objects such as circles (for pellets), as well as features such as the size of the circles (for estimating the mass of the cell). This hypothesis will be tested by comparing the performance of the pixel and semantic representations between a CNN with 3 convolutional layers to that of a CNN with 2 convolutional layers. The first network has the same structure as the one used in the 2015 DQN paper (Mnih et al., 2015). With the only difference being that the one used here only uses one single channel for the current representation of the game, whereas the one used by Mnih et al. use convolution over the 4 last frames. The second examined CNN has a similar structure to the 2013 DQN paper (Mnih et al., 2013).

Furthermore, to emphasize how the semantic representation is used to achieve high performances with relatively small networks, the mentioned methods will also be compared to that of a standard MLP without convolutional layers that uses a semantic state representation of resolution 11 by 11.

4 EXPERIMENTAL SETUP

This research uses the OpenAI baselines repository (Dhariwal et al., 2017) for prioritized experience replay to enhance reproducibility. The hyperparameters have been tuned using a coarse search through parameter space and can be found in the appendix.

4.1 General Experimental Setup

In all experiments, the environment resets after 20,000 game steps. This is considered to be one episode. Upon reset the agent is reassigned a new cell with mass 10 at a random location and all pellet locations are randomized. This is done to avoid that the

learning agent learns peculiarities of pellet locations on the map and to force the agent to also learn to deal with low cell mass strategies. Furthermore, to avoid the network from overfitting to one particular color in the pixel value representations, we also have the player cell color randomized every time an episode ends. Pellet colors are always randomized when new pellets are generated in the game.

Each algorithm instance was trained with 300,000 state transitions. Given the network used a frame skip rate of 10, one state transition experience was generated every 11 in-game frames, giving a total of 3,300,000 game steps. These states were generated on-line as the network learned to play and stored into the experience replay buffer of size 20,000. Every training step, the network was trained on 32 experiences sampled (with replacement) from a single batch. On an Intel Xeon E5 2680v3 CPU @2.5Ghz it took between 32 to 84 hours to train each individual CNN run depending on the trial. State representations of 42 by 42 in resolution were at the lower end due to their smaller amount of network parameters, while resolutions of 84 by 84 took the longest to train on. On the other hand, the MLP runs took approximately 5.5 hours.

Every 5% of the training process the performance of one agent is tested five times. The noise factor of the agent (ϵ of ϵ -greedy) is then set to zero. In this environment the agent collects pellets for 15,000 in-game steps. Furthermore, after training is completed the agent is placed in the environment 10 times to measure the final performance.

A simulation refers to the complete training and testing process as described before. The performances for each experimental condition are calculated by taking the mean scores from 10 independent simulations.

4.2 Network Structures

The simple MLP architecture consists of a variable input length, 3 fully connected layers, and an output layer. All artificial neural networks were constructed using Keras 2.1.4 (Chollet et al., 2015). The input to the MLP consists of the grid of the semantic representation, which was first flattened into a 1D vector, and then had 2 extra values appended to it: the current mass of the player, and the 'field of view' (FoV) size of the player. These two extra values are information the human player has implicit access to in the real game through estimation of the total mass and FoV size by comparison to features such as the relative sizes of a food pellet, or the game background. This source of information is useful, as the optimal

strategy in the game changes depending on size. For a state's semantic representation resolution of 11 by 11 where a pellet vision grid is used, the 1D input vector of the network would be 123 in length. This input is then fed into 3 subsequent fully connected layers of 250 rectified linear units each. This is then followed by an output layer of 25 linear units which refer to the 25 possible actions. The output layer, as specified in the 'Reinforcement Learning' section, has units symbolizing the Q-value of a possible mouse position on the screen using a grid-like fashion (see Figure 1).

The first CNN architecture has the same structure as that used for Atari games in the 2015 DQN paper (Mnih et al., 2015), with the difference being that the structures used here only use the current frame in the input for the convolution. The default input consists of 84 by 84 units in length, the number of channels is dependent on the type of representation used. The first convolutional layer uses a kernel size of 8 by 8 with stride 4 for a total of 32 filters. The second convolutional layer uses a kernel size of 4 by 4 with stride 2 for 64 filters. The third convolutional layer uses a kernel size of 3 with stride 1 for 64 filters. Every convolutional layer applies a rectified linear activation function. At this point in the network, the current layer's output was flattened and, similar to the case of the MLP's input, the values for the mass of the player and the FoV size were appended to it. Next, this 1D vector was fed to a fully connected layer of 512 rectifier units, which was then followed by an output layer of 25 linear units.

Lastly, the second CNN architecture has a similar structure to the first one, but has only 2 convolutional layers. Again, the input by default consists of 84 by 84 units in length. The number of channels is dependent on the type of representation used. The first convolutional layer uses a kernel size of 8 by 8 with stride 4 and a total of 32 filters. The second convolutional layer uses a kernel size of 4 by 4 with stride 2 and 64 filters. Every convolutional layer applies a rectified linear activation function. Just like in the other CNN architecture, at this point the layer's output is flattened into a 1D array and gets appended the mass and FoV player values. Next, a fully connected layer of 256 rectifier units is used, which is then followed by an output layer of 25 linear units.

5 EXPERIMENTAL RESULTS

5.1 General Results

Figure 4 shows the test results with different resolutions for the vision grid representation using both

CNN architectures. The 42 by 42 resolutions perform better than every other resolution. The 84 by 84 resolution performs the second best closely followed by the 63 by 63 resolution. Unsurprisingly, as seen in Figure 5, the 42 by 42 resolution also achieves good training performances the fastest due to its lower number of trainable parameters. The 3 convolutional layer network seems to also achieve slightly better performances than the 2 convolutional layer CNN for resolutions of 42 by 42 and 63 by 63, but not for 84 by 84. The MLP architecture with the 11 by 11 resolution seems to achieve a higher performance than both CNNs using 84 by 84 resolutions, although not as high as CNNs using 42 by 42 resolutions. The MLP seems to learn at a similar rate as 84 by 84 CNN resolutions (see Figure 5).

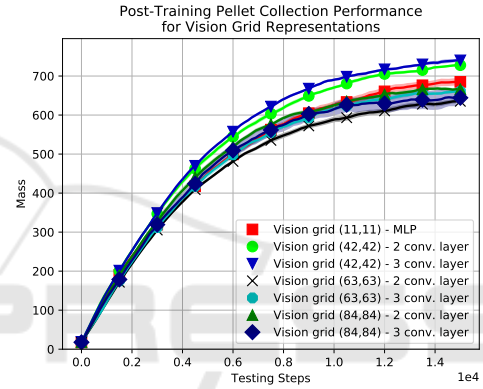


Figure 4: Post-training performance of vision grid representations with differing resolutions for the two CNN architectures, as well as for the MLP architecture with a 11 by 11 resolution. Each point represents the average of the 10 testing rounds and the shaded area denotes its 1 standard error (SE) range. Results are averages of 10 simulations.

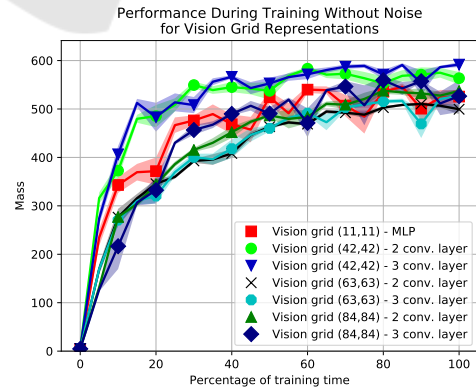


Figure 5: During-training performance of vision grid representations with differing resolutions for the two CNN architectures, as well as for the MLP architecture with a 11 by 11 resolution. Each point represents the average of the 5 testing rounds and the shaded area denotes its 1 SE range.

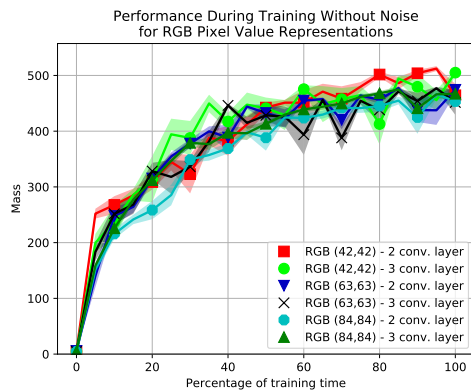


Figure 6: During-training performance of RGB pixel value representations with differing resolutions for the two CNN architectures. Each point represents the average of the 5 testing rounds and the shaded area denotes its 1 SE range.

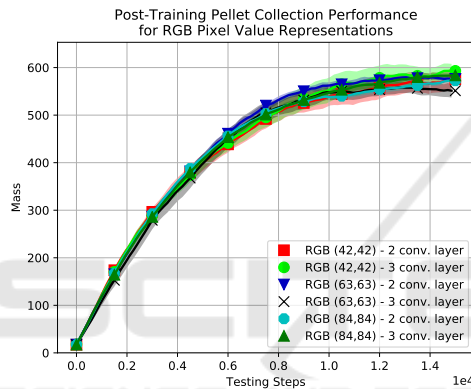


Figure 7: Post-training performance of RGB pixel value representations with differing resolutions for the two CNN architectures. Each point represents the average of the 10 testing rounds and the shaded area denotes its 1 SE range.

The RGB pixel value representations seem to all have similar during-training performances as seen in Figure 6, suggesting that resolution does not have much of an effect on the learning process of the networks for the resolutions tested with RGB pixel values. This is further emphasized by Figure 7, where there are no noticeable differences between the resolutions or architectures in post-training performance.

Lastly, the grayscale pixel value representation appears to have trends similar to those of vision grids, but not to the same extent. The during training performance of the 42 by 42 resolutions seems to converge at a slightly higher performance than the other 2 resolutions (see Figure 8). The post-training performance seen in Figure 9 also seems to indicate that 42 by 42 resolutions have a higher performance after 300,000 training steps.

In order to observe how different kinds of state representations compare to one another, some of the

highest performing runs were plotted together as seen in Figures 10 and 11. The best results are obtained with the vision grids with resolution 42×42 . The 42 by 42 grayscale representation on a 2 convolutional layer network seems to achieve a similar final performance as both 84 by 84 vision grid representations. This grayscale run is noticeably better than the plotted 42 by 42 RGB representation with a 3 convolutional layer network in terms of final performance.

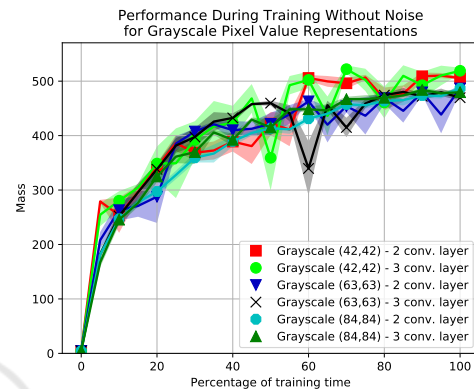


Figure 8: During-training performance of grayscale pixel value representations with differing resolutions for the two CNN architectures. Each point represents the average of the 5 testing rounds and the shaded area denotes its 1 SE range.

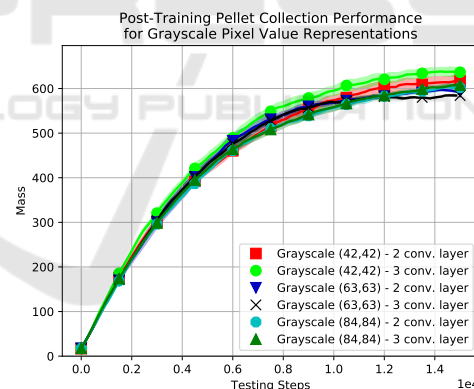


Figure 9: Post-training performance of grayscale pixel value representations with differing resolutions for the two CNN architectures. Each point represents the average of the 10 testing rounds and the shaded area denotes its 1 SE range.

The post-training performances for all conditions are listed in Table 1. The column 'Mean Performance' shows the mean testing scores across all 10 tests of all 10 simulations. The column 'Mean Max Performance' shows the average maximum scores across all 10 tests of all 10 simulations. The top scoring condition appears to be 'Vision grid (42,42) - 3 conv. layers' with a max score of 763. Comparing its max score to its 2 convolutional layer counterpart (which

Table 1: Post-training mean performances across 10 simulations. The 'Mean Performance' column contains the mean mass value for the post-training averaged performance curve. The 'Mean Max Performance' column shows the max scores of the post-training averaged performance curve.

	Mean Performance	Std. Error Mean	Mean Max Performance	Std. Error Max
Random	18	0.1	31	0.2
Greedy Heuristic	527	0.3	693	0.6
Vision grid (11,11) MLP	481	2.8	704	5.9
Vision grid (42,42) 3 conv. layer	537	0.6	763	0.9
Vision grid (42,42) 2 conv. layer	526	1.1	750	1.1
Vision grid (63,63) 3 conv. layer	479	1.3	688	0.6
Vision grid (63,63) 2 conv. layer	461	1.4	662	1.8
Vision grid (84,84) 3 conv. layer	480	5.7	675	5.4
Vision grid (84,84) 2 conv. layer	494	1.2	696	1.1
Grayscale (42,42) 3 conv. layer	471	4.2	669	4.9
Grayscale (42,42) 2 conv. layer	449	4.5	648	6.8
Grayscale (63,63) 3 conv. layer	446	2.0	617	1.2
Grayscale (63,63) 2 conv. layer	448	3.1	625	1.1
Grayscale (84,84) 3 conv. layer	442	2.1	632	1.7
Grayscale (84,84) 2 conv. layer	439	1.5	627	2.2
RGB (42,42) 3 conv. layer	432	7.2	628	6.8
RGB (42,42) 2 conv. layer	425	7.0	609	9.9
RGB (63,63) 3 conv. layer	421	7.8	588	7.4
RGB (63,63) 2 conv. layer	436	2.3	609	2.7
RGB (84,84) 3 conv. layer	421	7.8	588	7.4
RGB (84,84) 2 conv. layer	427	0.9	598	1.6

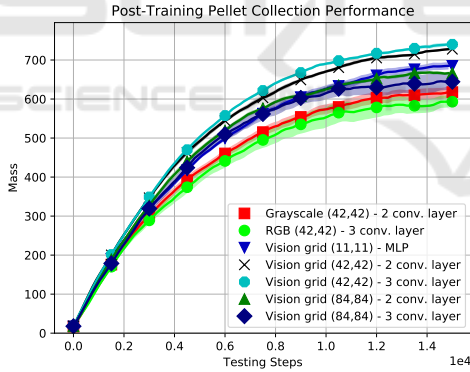


Figure 10: Post-training performance of various top-performing runs of various representations and network architectures. Each point represents the average of the 10 testing rounds and the shaded area denotes its 1 SE range.

holds the second highest score) through the use of a t-test yields a p-value of 0.019, suggesting there is a significant difference between their maximum scores. This method also significantly outperforms the Greedy bot and the vision grid with the MLP.

5.2 Discussion

As seen in Figures 10 and 11, the best performances are achieved by the CNN networks using vision grid

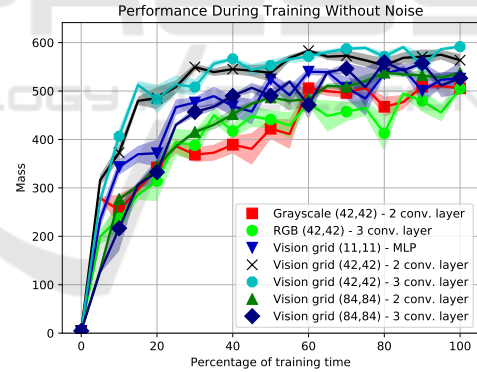


Figure 11: During-training performance of various top-performing runs of various representations and network architectures. Each point represents the average of the 5 testing rounds and the shaded area denotes its 1 SE range.

representations. Although the MLP network achieves a surprising performance despite its requirement of having a low resolution state representation, both CNN architectures using the vision grid with a 42 by 42 resolution reach a higher performance at a faster pace.

The performance increase in relation to the MLP is likely due to the CNNs' increased ability to process local changes in the environment, thus not having to evaluate potentially uncorrelated inputs far apart in

the network's input. This also allows a CNN to have a higher resolution input while keeping its number of parameters low, which helps explain why CNNs reach higher performances faster than the MLP. The deeper CNN architecture at 42 by 42 input resolution has 118,969 trainable parameters while the MLP architecture has 169,753.

The semantic representations yield a surprising performance in comparison to the RGB and grayscale pixel values. Even at resolutions of 11 by 11, the MLP yields a significantly higher performance than using RGB or grayscale pixel inputs. It should be noted that the pixel value representations have not fully converged after 300,000 training steps (see Figure 11), and that it could be the case that given enough training time, these could match the performance of vision grids. The same conclusion can be drawn for higher vision grid resolutions (particularly 84 by 84), which by the end of the training period have also not converged.

A reason that could explain why the 63 by 63 resolutions performed worse, is that the input dimensions are odd-numbered while the kernel strides are even. This causes the network to ignore 3 columns on the right of the input and 3 columns on the bottom of the input, leading to a loss of possibly important information.

6 CONCLUSION

Deep reinforcement learning has obtained many successes for optimizing the behavior of an agent with pixel information as input. This paper focused on using deep reinforcement learning for the pellet collection task in the game Agar.io. We researched different types of state representations and their influence on the learning process of the Q-learning algorithm combined with deep neural networks. Furthermore, different resolutions of these state representations have been examined and combined with different artificial neural network architectures.

The results show that the use of a vision grid representation, which transforms raw pixel inputs to a more meaningful representation, helps to improve training speed and final performance of the deep Q-network. Furthermore, a lower resolution (of 42×42) for both the vision grid representation and the raw pixel inputs leads to higher performances. Finally, the results show that a convolutional neural network with 3 convolutional layers generally outperforms a smaller CNN with 2 convolutional layers.

In future work, we aim to extend the algorithm so that the agent learns to play the full game of Agar.io.

For this it would also be interesting to use the sampled policy gradient (SPG) algorithm from (Wiehe et al., 2018) and combine it with the used methods from this paper. Finally, we want to compare the deep Q-network approach from this paper to Deep Quality-Value (DQV)-Learning (Sabatelli et al., 2018) for learning to play the game Agar.io.

ACKNOWLEDGMENTS

We would like to thank the Center for Information Technology of the University of Groningen for their support and for providing access to the Peregrine high performance computing cluster.

REFERENCES

- Bom, L., Henken, R., and Wiering, M. A. (2013). Reinforcement learning to train Ms. Pac-Man using higher-order action-relative inputs. In *Adaptive Dynamic Programming and Reinforcement Learning (ADPRL)*, pages 156–163.
- Chollet, F. et al. (2015). Keras.
- Dhariwal, P., Hesse, C., Klimov, O., Nichol, A., Plappert, M., Radford, A., Schulman, J., Sidor, S., and Wu, Y. (2017). OpenAI baselines.
- Hasselt, H. V. (2010). Double Q-learning. In *Neural Information Processing Systems (NIPS)*, pages 2613–2621. Curran Associates, Inc.
- Hochreiter, S. and Schmidhuber, J. (1997). Long Short-Term Memory. *Neural Computation*, 9(8):1735–1780.
- Knegt, S. J. L., Drugan, M. M., and Wiering, M. A. (2018). Opponent modelling in the game of Tron using reinforcement learning. In *International Conference on Agents and Artificial Intelligence (ICAART)*, pages 29–40. SciTePress.
- Lample, G. and Chaplot, D. S. (2017). Playing FPS games with deep reinforcement learning. In *AAAI Conference on Artificial Intelligence*, pages 2140–2146.
- Lin, L.-J. (1992). Self-improving reactive agents based on reinforcement learning, planning and teaching. *Machine Learning*, 8(3):293–321.
- Mnih, V., Kavukcuoglu, K., Silver, D., Graves, A., Antonoglou, I., Wierstra, D., and Riedmiller, M. (2013). Playing atari with deep reinforcement learning. *arXiv preprint arXiv:1312.5602*.
- Mnih, V., Kavukcuoglu, K., Silver, D., Rusu, A. A., Veness, J., Bellemare, M. G., Graves, A., Riedmiller, M., Fidjeland, A. K., Ostrovski, G., et al. (2015). Human-level control through deep reinforcement learning. *Nature*, 518(7540):529.
- Sabatelli, M., Louppe, G., Geurts, P., and Wiering, M. A. (2018). Deep quality-value (DQV) learning. *ArXiv e-prints: 1810.00368*.

- Schaul, T., Quan, J., Antonoglou, I., and Silver, D. (2015). Prioritized Experience Replay. *ArXiv e-prints: 1511.0592*.
- Shantia., A., Begue, E., and Wiering, M. A. (2011). Connectionist reinforcement learning for intelligent unit micro management in Starcraft. In *International Joint Conference on Neural Networks (IJCNN)*, pages 1794–1801. IEEE.
- Sutton, R. S. and Barto, A. G. (2017). *Reinforcement Learning: An Introduction*. MIT Press.
- Tesauro, G. (1995). Temporal difference learning and TD-Gammon. *Communications of the ACM*, 38(3).
- Watkins, C. J. C. H. (1989). *Learning from Delayed Rewards*. PhD thesis, King’s College, Cambridge.
- Wiehe, A. O., Stolt Ansó, N., Drugan, M. M., and Wiering, M. A. (2018). Sampled Policy Gradient for Learning to Play the Game Agar.io. *ArXiv e-prints: 1809.05763*.

APPENDIX: HYPERPARAMETERS

Parameter	Value
Reset Environment After	20,000 training steps
Frame Skip Rate	10
Discount Factor	0.85
Total Training Steps	300,000
Optimizer	Adam
Loss Function	Mean-Squared Error
Weight Initializer	Glorot Uniform
Activation Function Hidden Layers	ReLU
Activation Function Output Layer	Linear
Prioritized Experience Replay Alpha	0.6
Prioritized Experience Replay Beta	0.4
Prioritized Experience Replay Capacity	20,000
Training Batch Length	32
Steps Between Target Network Updates	1500